CONF-970465--5 SAND97-0703C
SAND--97-0703C

Mine Detection Using Backscattered X-Ray Imaging Of AntiTank and AntiPersonnel Mines

Grant Lockwood*, Steve Shope, Luke Bishop, Michael Selph, John Jojola
Sandia National Laboratories, MS 1159, Albuquerque, NM 87185-1159

ABSTRACT

The use of backscattered X rays to image buried land mines and distinguish between surface and buried features has been well documented[1]. Laboratory imaging experiments, being conducted at Sandia National Laboratories/New Mexico (SNL/NM), have been used to develop preliminary data acquisition hardware and software for an upcoming Advanced Technology Demonstration (ATD). In addition image processing techniques, developed by the Department of Nuclear Engineering at the University of Florida (UF), are utilized.

Previous buried land mine imaging studies focused on antitank mines buried in screened sand and have included well defined surface features such as a board or a small diameter rock. In the present study we have examined imaging under a variety of practical environmental conditions. We have successfully imaged antitank mines (ATM) buried in sand and rocky New Mexico (NM) soil. Images have been obtained for bare surfaces as well as for surfaces covered with limestone road coarse base (gravel), snow, water, and native grass. In addition, we have imaged buried ATM and surface antipersonnel (AP) mines covered with debris consisting of various size rocks, a log, and leaves such that no mine was visible to the eye. Contour plots of the images obtained for the various environmental conditions are presented.

Keywords: backscattered X ray, imaging, mine detection, antitank mine, antipersonnel mine, land mine.

1. INTRODUCTION

The U.S. Army has a requirement for a vehicle-mounted detection system using backscattered X rays to image buried plastic antitank mines (PATM). It is hoped such a system could be developed to clear a 3-m-wide path through a mine field at a rate of 4.8 km/h to allow armor to breach the mine field quickly and safely. A mobile, continuously-scanning, x-ray machine (MCSXM) is being developed for this purpose[2]. This machine is scheduled to be demonstrated at an upcoming ATD. The SNL/NM Mine Detection Team has conducted a series of tests to develop a high-throughput Data Acquisition System (DAS) for use on the ATD. The x-ray machine for use on the ATD is not yet fully functional. Because of this, the DAS is being developed using the laboratory simulation system consisting of a Magnaflux x-ray machine and a computer-controlled soilbox.

Section 2 presents the apparatus used and the procedures developed for land mine image acquisition. Acquired images are displayed as contour plots in Section 3. The results will be discussed and our conclusions will be given in Section 4.

2. APPARATUS AND PROCEDURES

To simulate the MCSXM to be deployed in the ATD, a laboratory-based, automated-scanning system was developed. The laboratory system consists of a 122-cm by 122-cm by 30.5-cm-deep soilbox mounted to a single-axis, programmable motion table. The motion in the second dimension is currently implemented with a remote hand crank to move the x-ray machine perpendicular to the soilbox motion. The x-ray source is a 150-kV (max), 5-mA (max) commercial source manufactured by Magnaflux. The source generates steady state x-ray pulses at 1.8-ms periods with an approximate Full-Width-Half-Max (FWHM) of 400 μs. The spot size at the ground surface is approximately 2 cm in diameter. The spot size determines the minimal spatial resolution of the system. The source spot size was matched as close as possible with the MCSXM collimated size to allow comparable studies of object resolution. The laboratory simulation system allows for in-depth studies of source energies, source flux, possible scanning rates, as well as a detailed study the imaging algorithms. A central area (80 cm by 80 cm) was used to limit scattering from the soilbox walls. The electron-beam current, used to generate X rays in the laboratory x-ray machine, is only a fraction of the current produced in the MCSXM. We chose as a figure of

*.(Further author information -

G. L (correspondence): E-mail: gjlockw@sandia.gov; Telephone: 505.845.7007. Fax: 505.845.7244.

DISCLAIMER

merit, for the laboratory simulation, the electron-beam current multiplied by the time required to obtain an image data point. The time to move the soilbox 80 cm was adjusted to make the figure of merit approximately equal to that of the MCSXM.

The x-ray source/detector configuration, used to make the backscattered x-ray measurements, is shown in Figure 1. With this arrangement, the use of two sets of detectors gives a stereoscopic view and depth information. The uncollimated detectors (UD) primarily detect surface features while the collimated detectors (CD) detect both surface and buried objects. Thus, the subtraction of UD from CD should remove most surface features leaving an image of a buried object. For the simulation, we used the actual MCSXM detectors. These consisted of 2 each 7.6-cm-wide uncollimated detectors and 2 each 30.5-cm-wide collimated detectors. Each detector consists of 5.8-cm-thick by 244-cm-long plastic scintillator with a photomultiplier tube on each end. However, the group, working on the MCSXM, required the use of one of the detectors. This left one 30.5-cm and two 7.6-cm detectors to use in developing the DAS.

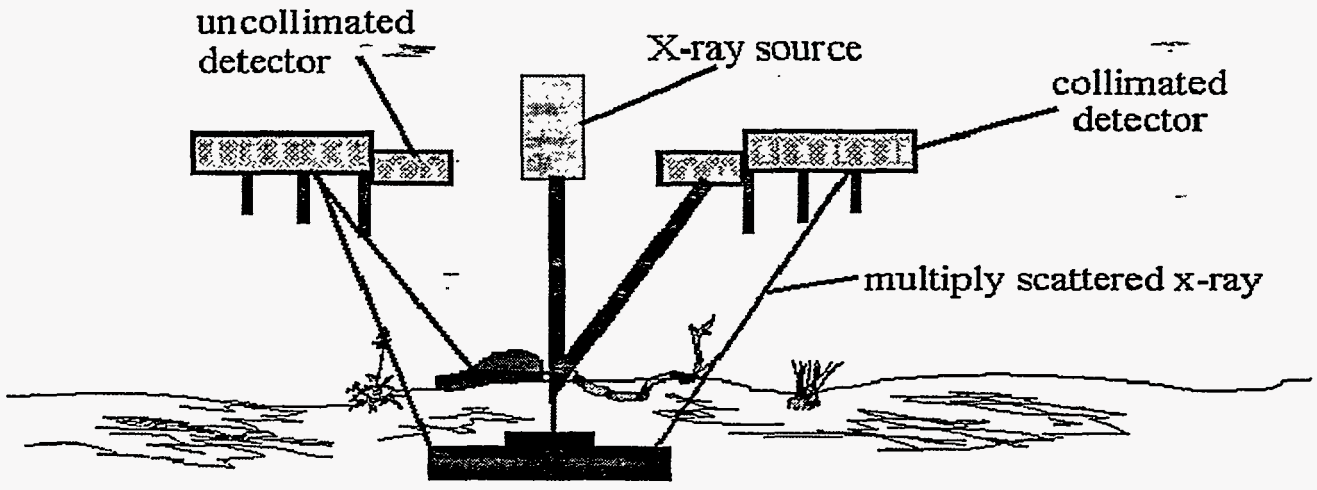

Figure 1: Application of backscattered X rays to detect buried plastic mines and remove surface clutter.

At the start of the test series we obtained data using two uncollimated detectors and one collimated detector. With this arrangement some of the final images were asymmetric due to the use of only one collimated detector. To verify that this was indeed the problem we used one of the 7.6-cm-detectors as a partial collimated detector. By recording the signals from the 30.5-cm collimated detector and the 7.6-cm 'collimated' detector on separate channels, normalizing and summing the results we obtained a near symmetric image as shown in Figure 2.

The preliminary x-ray detector data acquisition system is shown in figure 3. Note that all four detectors are shown in the figure.

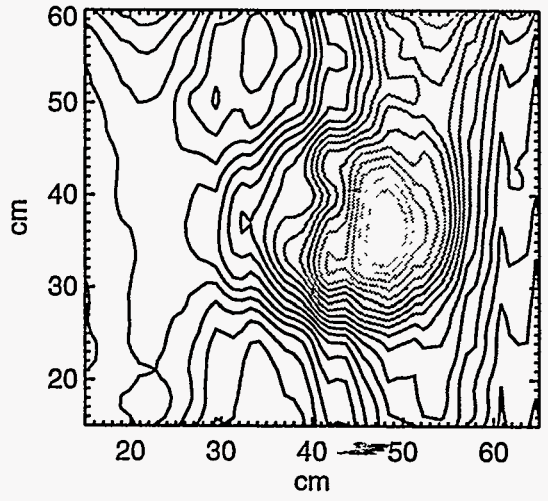

Figure 2a

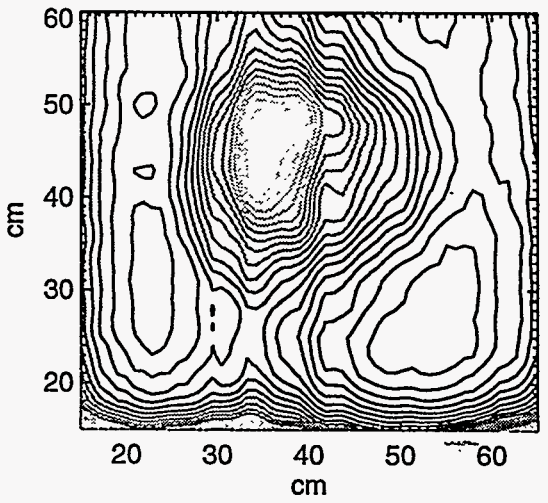

Figure 2b

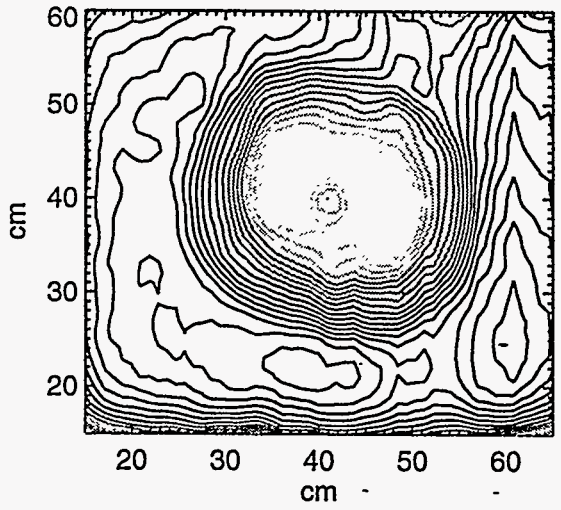

Figure 2c

Figure 2: Image of 30-cm (diameter) PATM in rocky NM soil (depth-of-burial is 2.54 cm). Figure 2a is the image obtained from the 30.5-cm-wide collimated detector. Figure 2b is the image obtained from the 7.6-cm- wide detector (also collimated). Figure 2c is a symmetric image of the mine obtained by adding the normalized (4.22) 7.6-cm detector signal to that of the 30.5-cm detector signal.

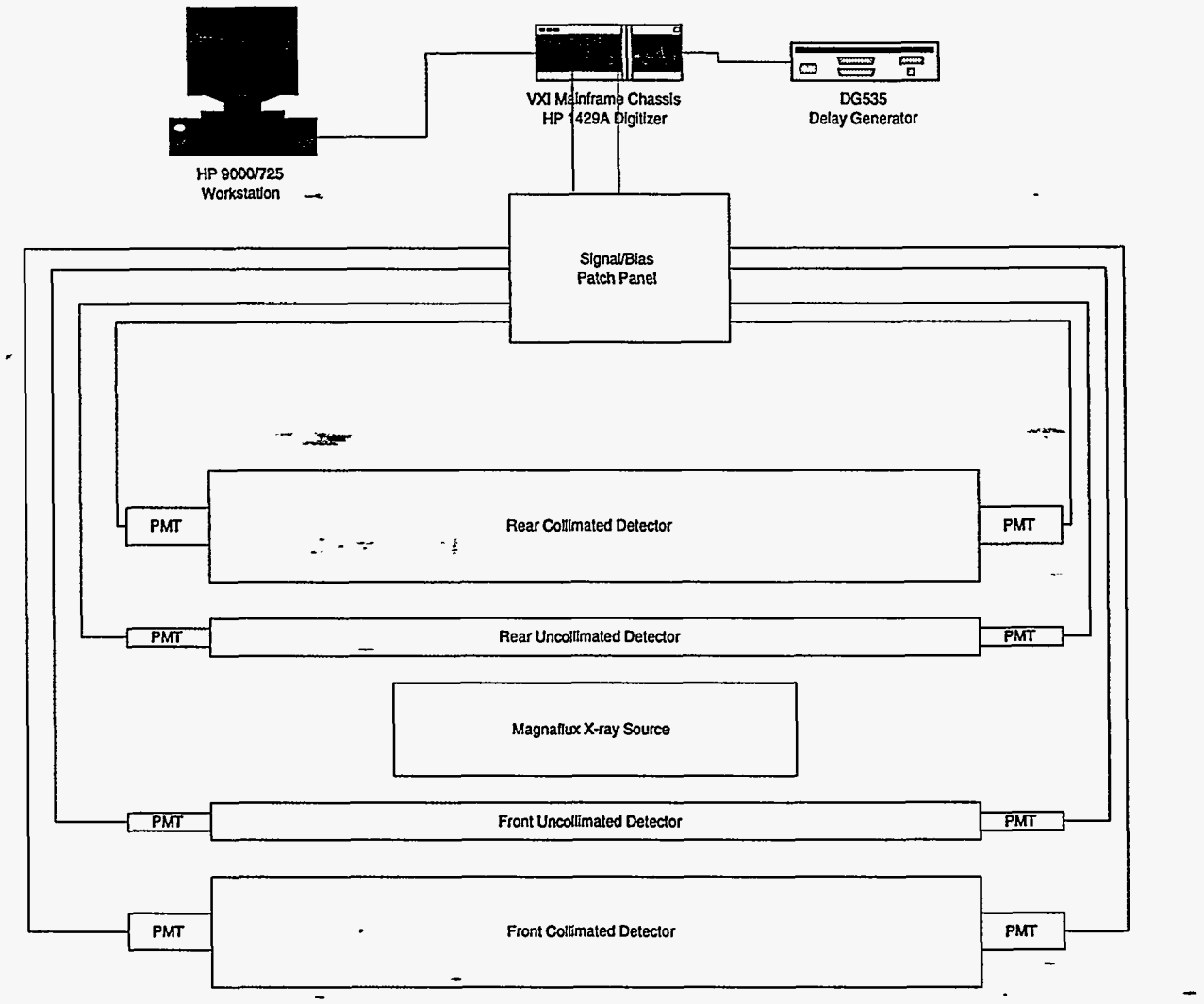

Figure 3: Laboratory Simulation System Diagram

A Hewlett-Packard (HP) 12-bit, 2-channel VXI-based, programmable digitizer (HP E1429A) is configured to acquire many (1024) equally-spaced segments or snapshots of the collimated and uncollimated detector signals as the soilbox is moved continuously under the x-ray source. The HP E1429A digitizer is programmed at the VXI register level to enable very fast data transfer rates to the host computer. As configured, data can be transferred from the digitizer to the host computer at a rate of 500k readings (16 bit words) per second. Up to 2M readings/second are possible when an embedded computer is used in the VXI mainframe chassis. Detector signals are routed to high-impedance, differential inputs of the HP E1429A digitizer via high-quality coaxial signal cable. For the laboratory simulation system, each acquisition segment is set to 20 ms in duration with a record length of 1024 samples, thus acquiring a waveform of approximately 12 each 400-μs (FWHM) pulses of the x-ray source. A simple integration method is applied to the entire 20 ms window and the integral value is extracted and stored as relative intensity value of the detected signal. By integrating multiple source-output pulses the pulse-to-pulse variations that the Magnaflux x-ray source exhibits are minimized. The resultant images are visually improved and the signal dynamic range is significantly improved. By limiting the signal processing to a simple integration, the processing time of each scan is minimal, maintaining a rapid turn-around rate between image scans.

Along a single scan, 80 segments are acquired and processed. An external, programmable delay generator (Stanford Research DG535) synchronizes the digitizer to the motion rate of the soilbox. For these tests, the DG535 is configured to output continuous bursts of pulses at a rate of 35.5 Hz (every 28.2 ms). The DG535 burst output causes the HP 1429A to re-

arm and acquire a scan segment every 28.2 ms. The delay generator also controls the start-of-motion of the programmable axis motion controller. The use of an external delay generator provides a flexible means of synchronizing the soilbox motion rate with the data acquisition rate. If a higher soilbox motion velocity is desired, the burst rate of the delay generator can be programmed to generate a faster digitizer re-arm rate. A total of 80 scans are acquired, processed, and stored to generate an 80 cm by 80 cm image of the soilbox contents. The image processing utilizes the UF-developed image enhancement algorithms[1].

The UF algorithms perform a 'globbing' technique that visually enhances the detected surface or buried object by identifying an object through the use of an adjacency matrix and uniformly scaling the amplitude of the adjacency matrix of each found object. The 'globbing' visualization technique was not used in the current research nor were any shape recognition methods applied to identify objects. The focus of the laboratory simulation studies has been to maximize detector responses and to statistically improve the acquired images through multiple, source-pulse integration, while scanning at real-life (i.e. ATD) rates. We have subtracted the uncollimated detector image from the normalized collimated detector image to produce buried feature images. The resultant images are displayed as color contour plots. Color contour plots provide the fastest, most intuitive perspective of surface and buried features. We have also employed the use of image slices or line-outs. A line-out is a cut across an image, fixing either the X or Y axis and displaying the full scan as a waveform plot. Line-outs provide additional detail information of object features, as well as a good visual indicator of dynamic range of the measurement. The data acquisition system, as it is currently developed, can be easily configured on the ATD system to acquire continuous, real-time-mode image data.

3. RESULTS

Using the DAS developed under this program, we have examined imaging of land mines under various realistic environmental conditions. The resulting images are shown as contour plots in Figures 4 through 8. Figure 9 shows the results of a high-resolution (slow scan rate) image of a "butterfly" antipersonnel mine. The figure shows an isometric view of the image and a line-out through the center of the mine. This figure is included to demonstrate the capability of the technique if slower scan rates could be employed or higher x-ray flux obtained.

All the images (except Figure 9), displayed in this section, were taken with a three detector arrangement (as discussed in Section 2) and thus the uncollimated and processed images are asymmetric. Amplitude information is generally lost due to the use of grayscale-only images shown in this paper. For laboratory simulation and for the ATD, high-resolution color contour plots are used to provide a fast, intuitive perspective of surface and buried features.

The processed images shown here were obtained by normalizing the collimated signal using the ratio of the signal levels obtained from line-out of the collimated and uncollimated detectors taken in a common, featureless area. These are denoted on the image plots by (constant * CD - UD). In these figures, CD and UD refer to the images generated by the one collimated detector and the two electrically-summed, uncollimated detectors, respectively. Note that only in the case where objects are above the buried mine is subtraction required to clearly show the mine shape as seen in Figure 8. In these figures, depth-of-burial (DOB) represents the thickness of material between the soil surface and the top surface of the buried mine.

In Figure 4 we show the images obtained from the collimated detector, the uncollimated detectors, and the processed image for two different test arrangements. The images in Figures 4a, 4b, 4c illustrate a PATM buried in rocky NM soil. The mine is clearly seen in the uncollimated image but is obscured (Figure 4e) after 2 cm of loose limestone road coarse base (gravel) was added. However, the mine is seen in both processed images (4c and 4f).

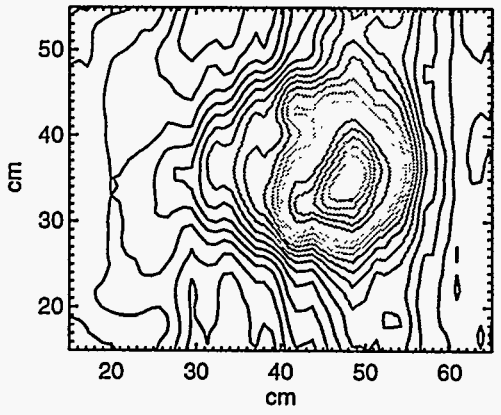

a. collimated

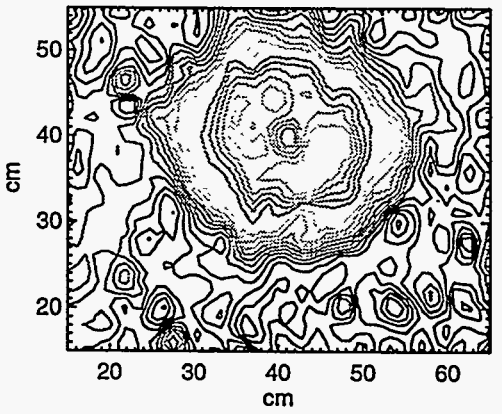

b. uncollimated

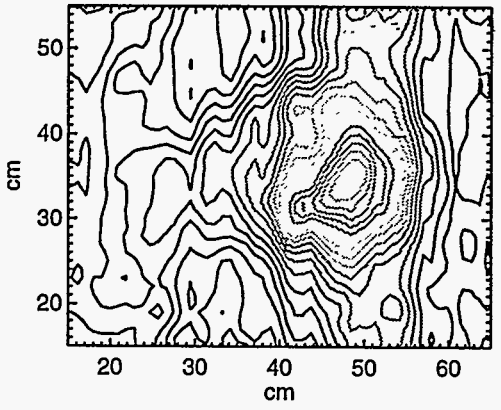

c. (7.64 * CD - UD)

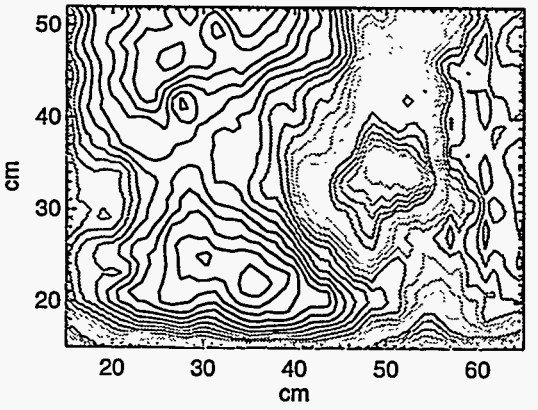

d. collimated (CD)

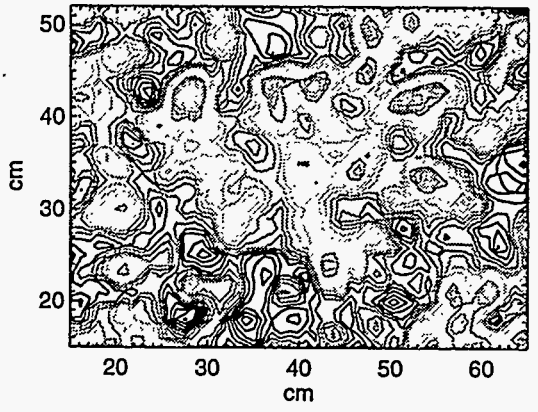

e. uncollimated (UD)

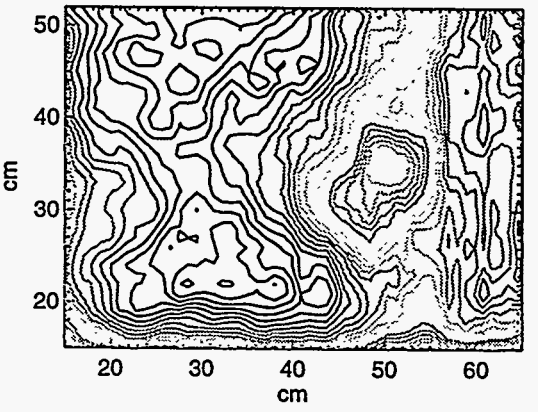

f. (9.4 * CD - UD)

Figure 4: Images of a 30 cm (diameter) PATM in rocky NM soil (DOB is 2.54 cm). In Figures 4d, 4e, and 4f an additional 2 cm of limestone road coarse base (gravel) was placed on top of the soil surface.

Figures 5 and 6 show the processed images of a buried PATM through various depths of snow and water, respectively. Note the snow used had a water content such that 1 cm of snow when melted produced 0.34 cm of water.

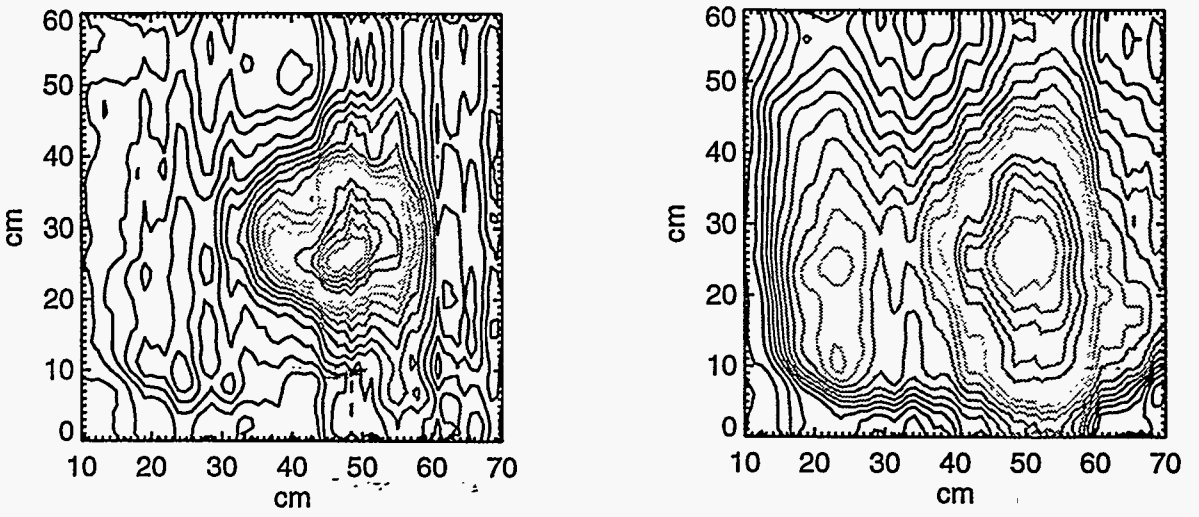

a. (10.7 * CD - UD) _ b. (10.2 * CD - UD)

Figure 5: Images of a 30 cm (diameter) PATM in sand (DOB is 1.0 cm). Image obtained through 2.54 cm of snow (Figure 5a) and 10.2 cm of snow (Figure 5b.

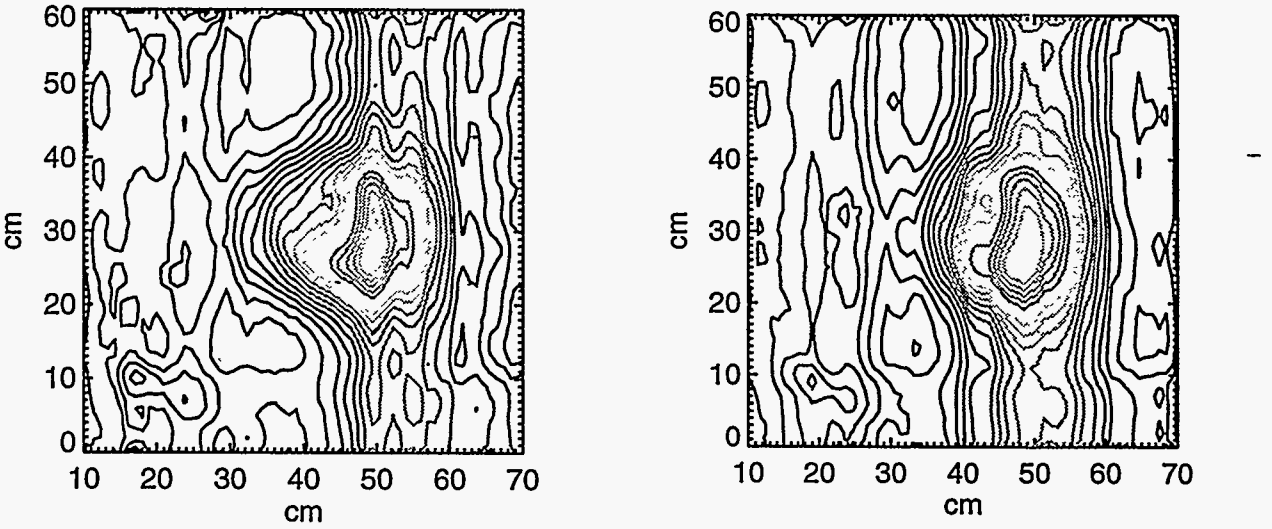

c. (12.8 CD - UD) d. (13.74 * CD - UD)

Figure 6: Images of a 30 cm (diameter) PATM in sand (DOB is 1.0 cm). Image obtained through 1.0 cm of water (Figure 6a) and 1.75 cm of water (Figure 6b).

Figure 7 demonstrates our ability to image a PATM buried among native grass sods. The dense root system of the sod is clearly seen in the uncollimated image (7c). These are removed by processing as seen in Figure 7d.

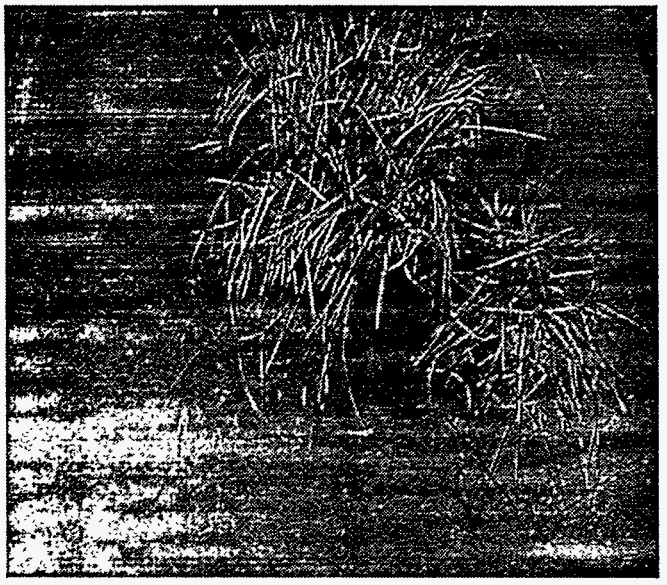

a. Test Arrangement_

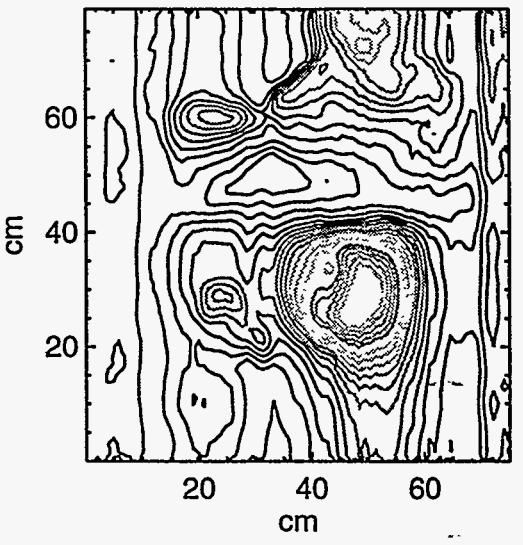

b. Collimated Detector (CD)

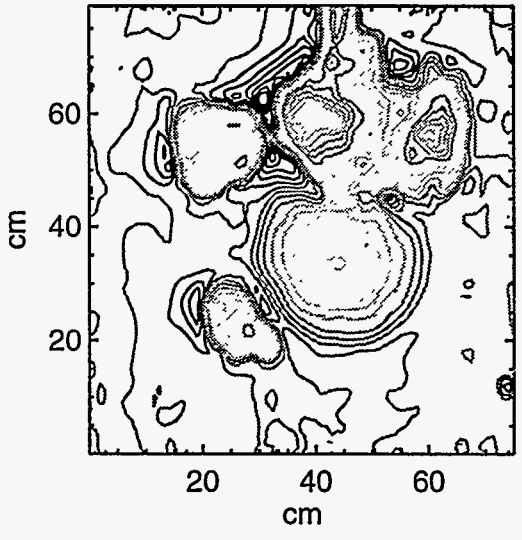

c. Uncollimated Detector (UD)

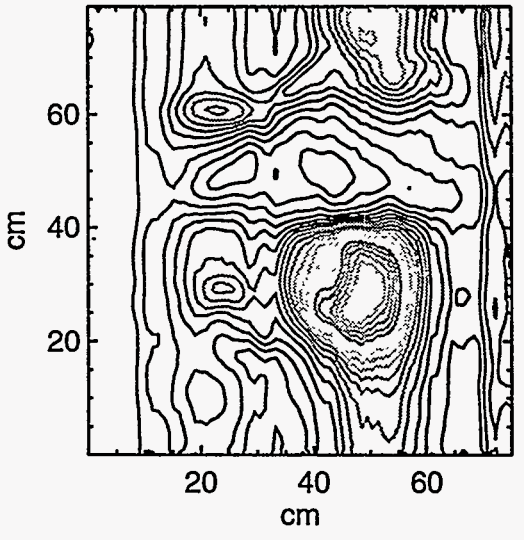

d. (13.3 * CD - UD)

Figure 7: Images of a 30 cm (diameter) PATM in sand (DOB is 1.0 cm). Images obtained with area planted with native grass sods. Figure 7a is a photo of the test arrangement.

Figure 8 presents the results when various mines and ground objects are imaged using this laboratory system. The test setup is shown in photograph 8a and the individual item identified. Photograph 8e shows how the test setup was obscured with leaves and grass prior to scanning the area of interest. In Figure 8b the two buried mines D and A are seen. The shape of mine D is distorted by the presence of log G and rock E. In the processed data (Figure 8d) the shape of mine D is clearly identified. Note that in this image (Figure 8d) the surface AP mine, the log and most of the rock are removed. If the presence of AP mines hidden by surface clutter (leaves) is important, they can be identified in Figure 8c by their shapes and signal amplitudes. As stated earlier, Figure 9 is included to demonstrate the resolution capabilities of this technique.

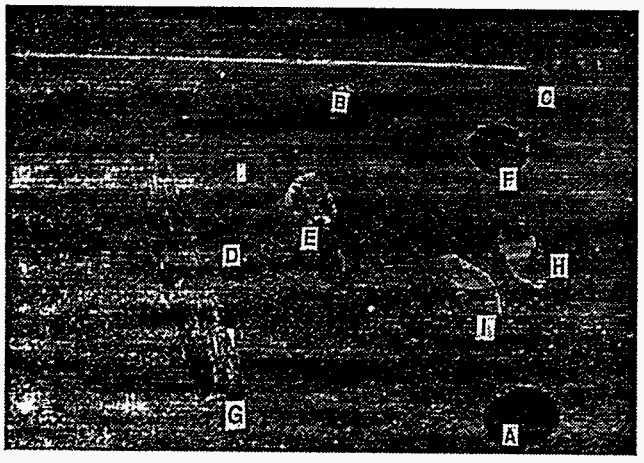

A. AP mine (PMN) DOB = 0 cm
B. Rock
C. Rock
D. 30 cm PATM (DOB = 2.54 cm)
E. Rock
F. AP mine (VS-MK2) on surface
G. Log
H. AP mine (PFM-1) "butterfly" on surface
I. Rock

a. Test Setup In Sand

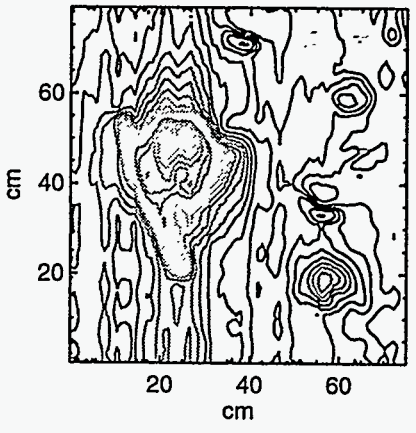

b. collimated detector (CD)

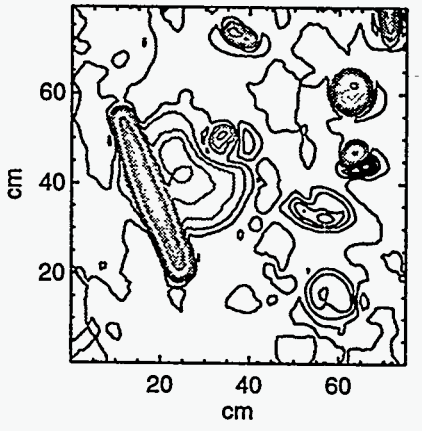

c. uncollimated detector (UD)-

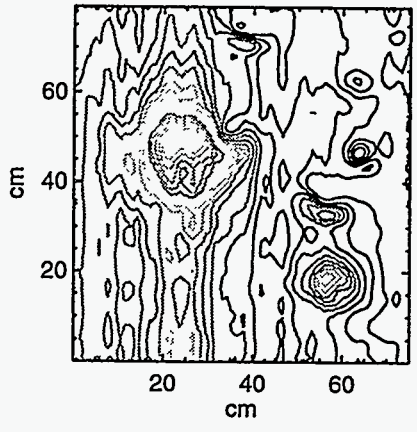

d. (12.3 * CD - UD)

e. Test Arrangement

Figure 8: Images of various mines and ground objects.The test setup and item identification are shown in 8a.

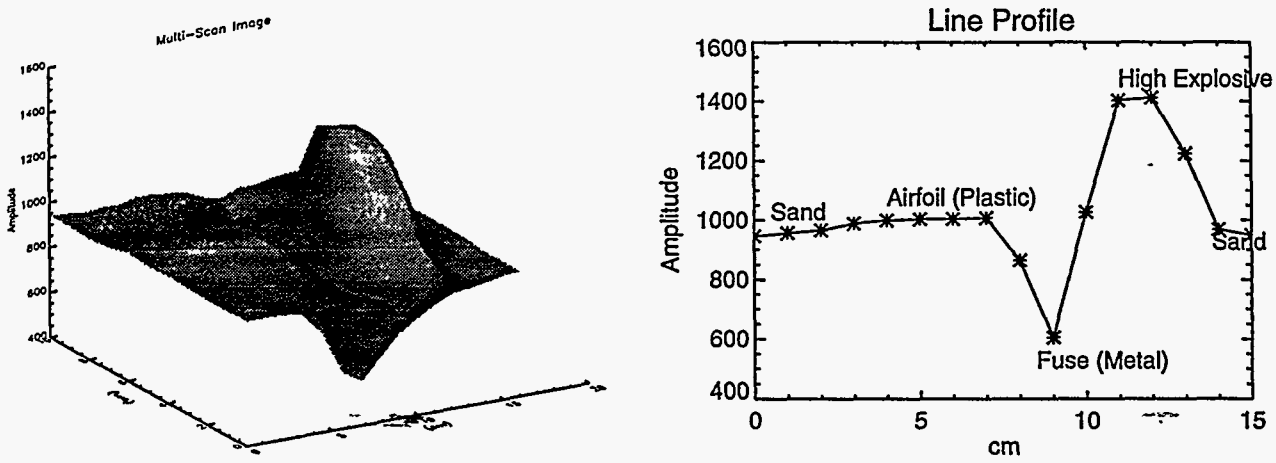

Figure 9: High resolution image of a "butterfly" antipersonnel mine (PFM-1) on surface covered with grass.

4. CONCLUSIONS

A high-throughput DAS has been developed which can easily be configured for the ATD. Using this DAS, with a laboratory simulation of the present ATD requirements, we have successfully imaged a variety of mines in various realistic environmental conditions. Additional laboratory studies should be conducted as the ATD requirements are finalized or altered. Further work is also needed to better define the limits of this technique. Final configuration of the DAS requires a fully functional MCSXM and will be completed in due course.

5. ACKNOWLEDGEMENTS

The authors would like to thank Charlotte Burchanowski of the Night Vision and Electromagnetic Sensor Division (NVESD) of the U.S. Army at Ft. Belvoir, VA. and Robert Moler of Systems Support, Inc. for their valuable technical advise and support. This program is funded by NVESD (MIPR7DDOE2717A) and a DoD/DOE Memorandum of Understanding.

6. REFERENCES

1. Wehlburg, J., Keshavmurthy, S., Watanabe, Y., Dugan, E., and Jacobs, A., "Image Restoration Techniques Using Compton Backscatter Imaging for the Detection of Buried Landmines.", SPIE Proceedings, Vol. 2496, p. 336-347 (1995).

2. Shope, S., Lockwood, G., Bishop, L., Selph, M., Jojola, J., Turman, B., "Mobile, Scanning, X-Ray Source for Mine Detection Using Backscattered X-Rays." (to be published in the proceedings of SPIE's 11th Annual International Symposium on Aerospace/Defense Sensing, Simulation, and Controls.").